P1.36 IMPACT OF MESOSCALE DATA, CLOUD ANALYSIS ON THE EXPLICIT PREDICTION OF AN MCS DURING IHOP 2002

Daniel T. Dawson II and Ming Xue*

School of Meteorology and Center for the Analysis and Prediction of Storms
University of Oklahoma

1. INTRODUCTION

As part of the International H_20 Project (IHOP_2002), which took place over the Southern Great Plains from 13 May to 25 June 2002, large amounts of high-resolution meteorological data were acquired or assembled from various observation platforms. These data, when assimilated into a numerical weather prediction (NWP) model, could potentially provide for improvements in forecasts of convective events over those that might be made using standard data sources. The goal of this study is to examine the impact of assimilating mesoscale data and the use of a complex cloud analysis scheme incorporating radar and satellite data on the explicit prediction of a severe mesoscale convective system (MCS) in the form of a bowing squall line. In this paper, a qualitative analysis of the predicted position of the MCS from various simulations starting with different initial conditions and at different horizontal resolutions is examined. Power spectra of 3-hourly accumulated precipitation will also be compared across the simulations.

The event took place on 15-16 June 2002. The MCS initially developed around 12Z on the 15th over central Nebraska and propagated southward, reaching northern Oklahoma around 0Z on the 16th. The system then continued southward through central Texas, reaching the Gulf Coast around 12Z on the 16th. Its path was marked by several reports of wind damage, and the MCS took on a distinct bow shape as it moved through Oklahoma (see Fig. 1).

2. METHODOLOGY

Analyses and simulations were performed for this event using the Advanced Regional Prediction System (ARPS) developed at the University of Oklahoma (Xue et al. 2000, 2003). The ARPS is a sophisticated numerical weather prediction (NWP) model that is capable of simulating a broad range of meteorological phenomena. Initial conditions for the simulations were produced using the ARPS Data Analysis System (ADAS), which uses an iterative analysis scheme that converges to the optimal interpolation (OI) solution (Brewster 1996; Case et al. 2002; Lazarus et al. 2002). The ADAS includes an optional complex cloud analysis scheme that utilizes satellite and radar observations to adjust the initial state of the model on convective scales (Zhang et al. 1998; Zhang 1999; Brewster 2001a,b; Souto et al. 2003).

The simulations herein were performed at three different nested horizontal resolutions, 27 km (covering the continental U.S.), 9 km, and 3 km, (see Fig. 2). The dimensions of the 9 km grid were 2250x2250x20 km^3, while that of the 3 km grid were 990x1800x20 km^3. Vertical grid stretching was employed in all simulations using 53 vertical levels starting with 20 m grid spacing in the low levels. All simulations were initialized at 12Z 15 June 2002 and were run out to 24 hours.

On the 9 km grid, four simulations, denoted 9km_alldata_c (the control run), 9km_alldata, 9km_standard, and 9km_eta, were performed. Table 1 summarizes the data used in the initial conditions for each of the simulations discussed herein. A new version of Kain-Fritsch convective parameterization was used in all the 9 km simulations. The surface mesonet data used in 9km_alldata_c and 9km_alldata included the Oklahoma Mesonet, the Southwest Kansas Mesonet, the Kansas Groundwater District #5 Mesonet, and the West Texas Mesonet. In the future, simulations with additional data sets available as part of the IHOP field program are planned. Also included in these two simulations were upper air data from the NOAA Profiler Network. 9km_standard included only SAO observations and the NWS upper air sounding network. Each of these three simulations used the same pre-existing real-time 27 km ARPS simulation that was produced during the IHOP program (Xue et al 2002) for the initial background field and for boundary conditions. Simulation 9km_eta was initialized via direct interpolation from a 27 km ARPS analysis grid that was in turn interpolated from the 12Z 15 June 2002 Eta analysis. Bound-

*Corresponding author address: Dr. Ming Xue, SOM, Sarkey's Energy Center, Room 1310, 100 E. Boyd St., Norman, OK 73019; mxue@ou.edu

ary conditions for 9km_eta were obtained from a 27 km simulation starting from the interpolated Eta initial conditions.

One 3 km simulation, denoted 3km_alldata_c, has been performed so far, with initial and boundary conditions interpolated from 9km_alldata_c, with no convective parameterization used. Other 3 km simulations are planned in which initial and boundary conditions taken from the other 9 km simulations mentioned previously will be used. Additional simulations at even higher resolutions (1 km) are also planned.

The large sizes of these computational grids require the use of parallel processing to obtain results in a reasonable time frame. The OSCER (OU Supercomputing Center for Education and Research) Linux Cluster was used for all simulations. A version of ARPS optimized for distributed-memory parallel processing using the MPI libraries was employed and jobs used up to 100 CPUs.

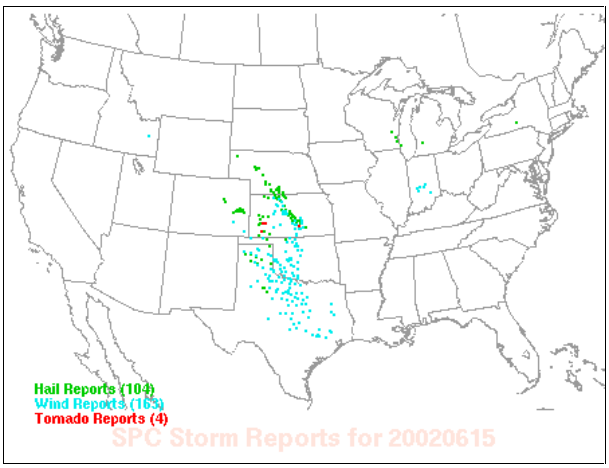

Figure 1. Storm Prediction Center (SPC) storm reports for 15 June 2002.

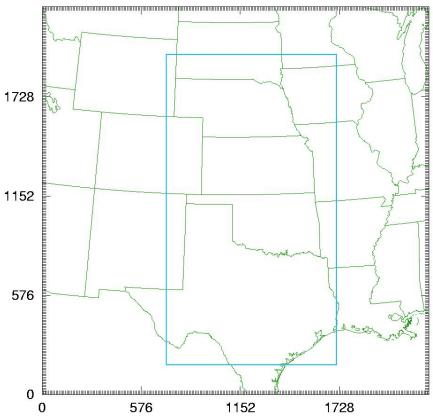

Figure 2. Computational domains for the 9 km (outer) and 3 km (inner) grids.

Table 1: List of Simulation Experiments

Simulation	Data Used
9km_alldata_c	NWS SAO surface observations, NWS upper air sounding network, surface mesonets, profilers, cloud analysis
9km_alldata	Same as 9km_alldata_c, except without the cloud analysis
9km_standard	NWS SAO surface observations, NWS upper air sounding network
9km_eta	Interpolated Eta analysis
3km_alldata_c	Interpolated from 9km_alldata_c, with additional cloud analysis

3. RESULTS

3.1. *Predicted Position of MCS*

To examine qualitatively the impact of the cloud analysis on the prediction of the position of the MCS, model simulated reflectivity at 3 hours into the simulations is examined. Figure 3 shows simulated composite radar reflectivity of the evolving MCS from each of the 9 km simulations at 3 hours, as well as the observed NEXRAD composite reflectivity at the same time. It can be seen from the figure that the use of the complex cloud analysis in the initial conditions (top left panel, simulation 9km_alldata_c) has a positive impact on the shape and position of the developing MCS, in that the system is elongated northwest to southeast and extends from north central Nebraska into north central Kansas as in the observed reflectivity (bottom center panel), while 9km_alldata and 9km_standard (top center and top right panels, respectively) both have a more circular-shaped system that lacks an extension into north central Nebraska. Interestingly and somewhat unexpectedly, 9km_eta (lower left panel) also shows a northwest to southeast oriented system with spotty convection that mimics the observed reflectivity even better than 9km_alldata_c, despite having been initialized with no cloud analysis or any additional data analysis on top of the interpolated Eta fields.

Figure 4 is as Fig. 3 except for 12 hours into the simulation (00Z on the 16th). By this time, the effect of the cloud analysis in the initial conditions has all but disappeared, as 9km_alldata_c and 9km_alldata have virtually identical systems. 9km_standard has a somewhat weaker system

that is shifted slightly south (~50 km) of 9km_alldata_c and 9km_alldata, while 9km_eta's system is shifted north (~50 km) and thus is the worst in the prediction of the position of the MCS. It should be noted that all the simulations are displaced somewhat east of the actual track of the system and are all too slow with the propagation, as the observed reflectivity shows the leading edge of the MCS has already moved into northern Oklahoma by this time, a position error of approximately 75 km for 9km_standard, 100 km for 9km_alldata_c and 9km_all_data, and 150 km for 9km_eta, measuring from the center of the leading edge of the bow echo between the simulations and observations. The convection in the Texas panhandle evident in the observed reflectivity is poorly represented by all of the 9km simulations. This convection formed earlier over southern Colorado (not shown) and propagated southeast, merging with the main MCS propagating southward out of Kansas at about the time of this figure. It is hypothesized that the lack of this convection within the 9 km simulations is at least partially responsible for the overall eastward displacement of the MCS relative to the observed system, in that this convection was important in strengthening the cold pool in the western portion of the MCS.

Figure 5 is as Fig. 3 except for 24 hours into the simulations (12Z on the 16th). 9km_alldata_c and 9km_alldata are again nearly identical, with 9km_standard showing a nearly identical in position but considerably weaker MCS. 9km_eta continues to be the worst in its portrayal of a weaker system that is displaced even further northeast than the three other simulations. The position error is now approximately 300 km in a northeast direction, for 9km_alldata_c, 9km_all_data, and 9km_standard, and approximately 400 km for 9km_eta.

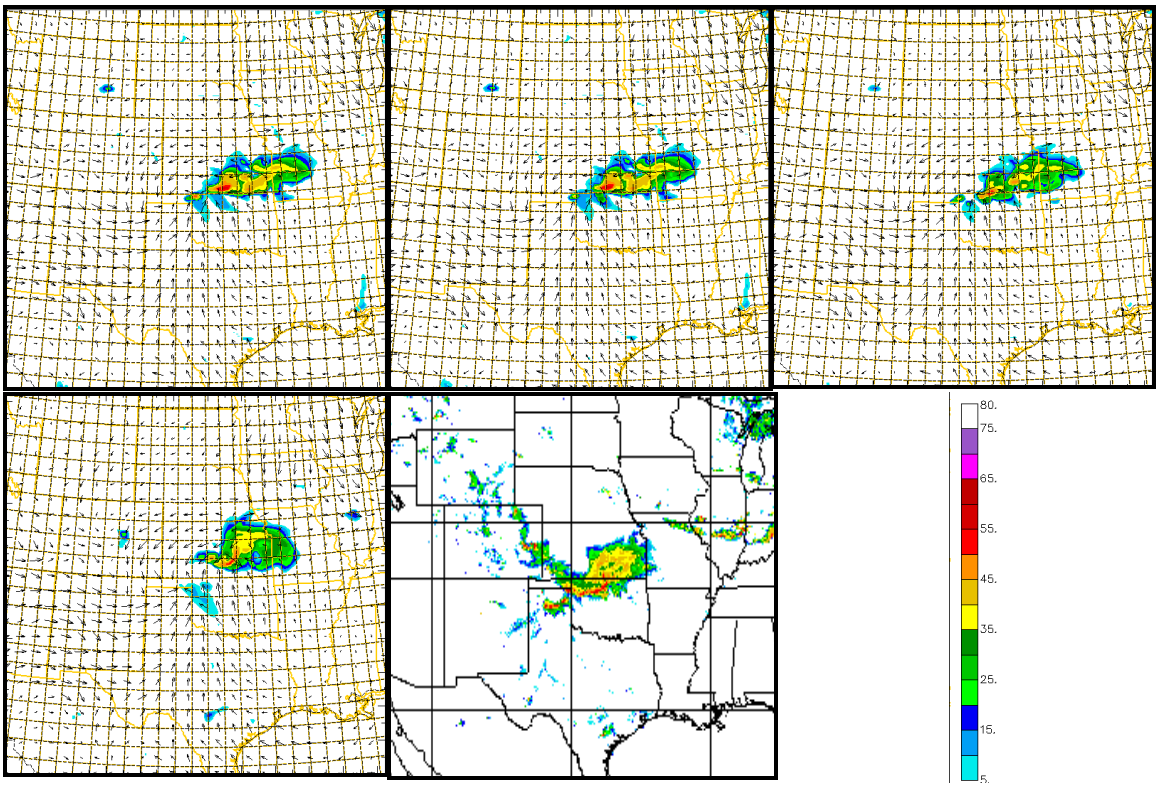

Fig. 3. Simulated composite reflectivity at 15Z 15 June 2002 (3 hr forecast) for 9km_alldata_c (top left), 9km_alldata (top center), 9km_standard (top right), and 9km_eta (bottom left). Also shown is the composite reflectivity from the NEXRAD Doppler Radar network at the same time.

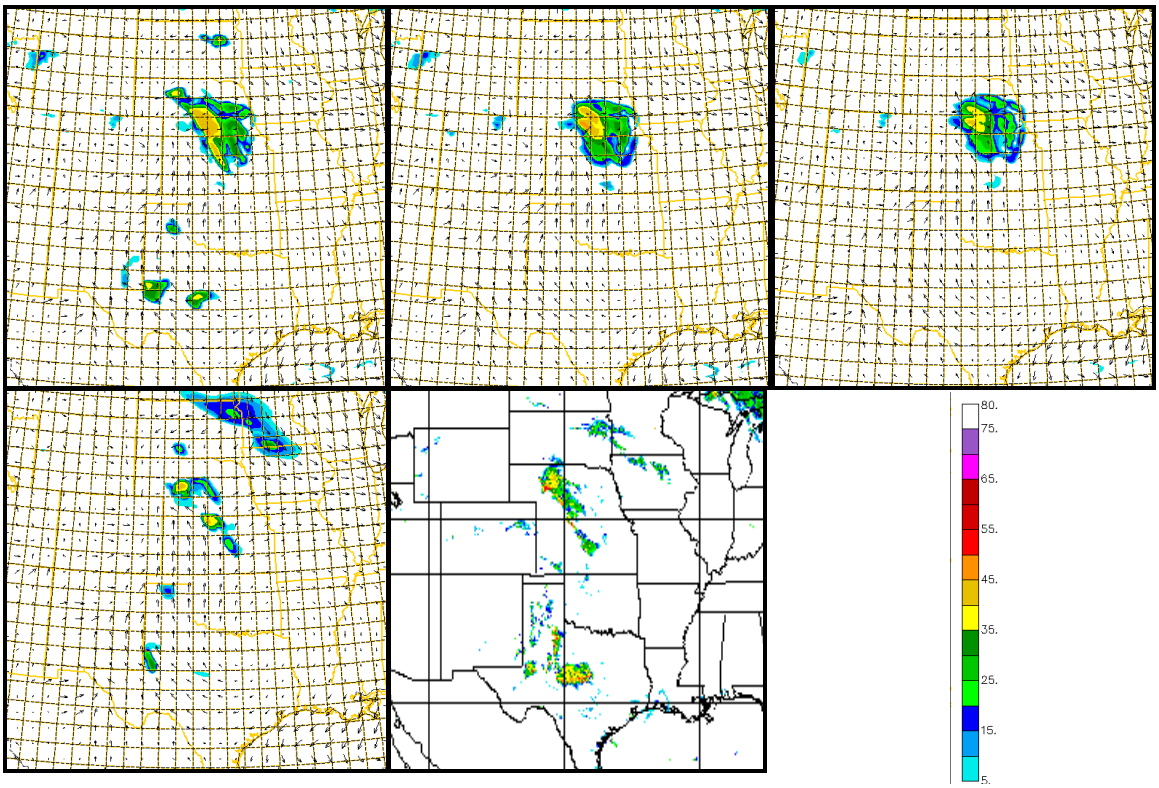

Fig. 4. As in Fig. 3 but for 00Z 16 June 2002 (12 hr forecast)

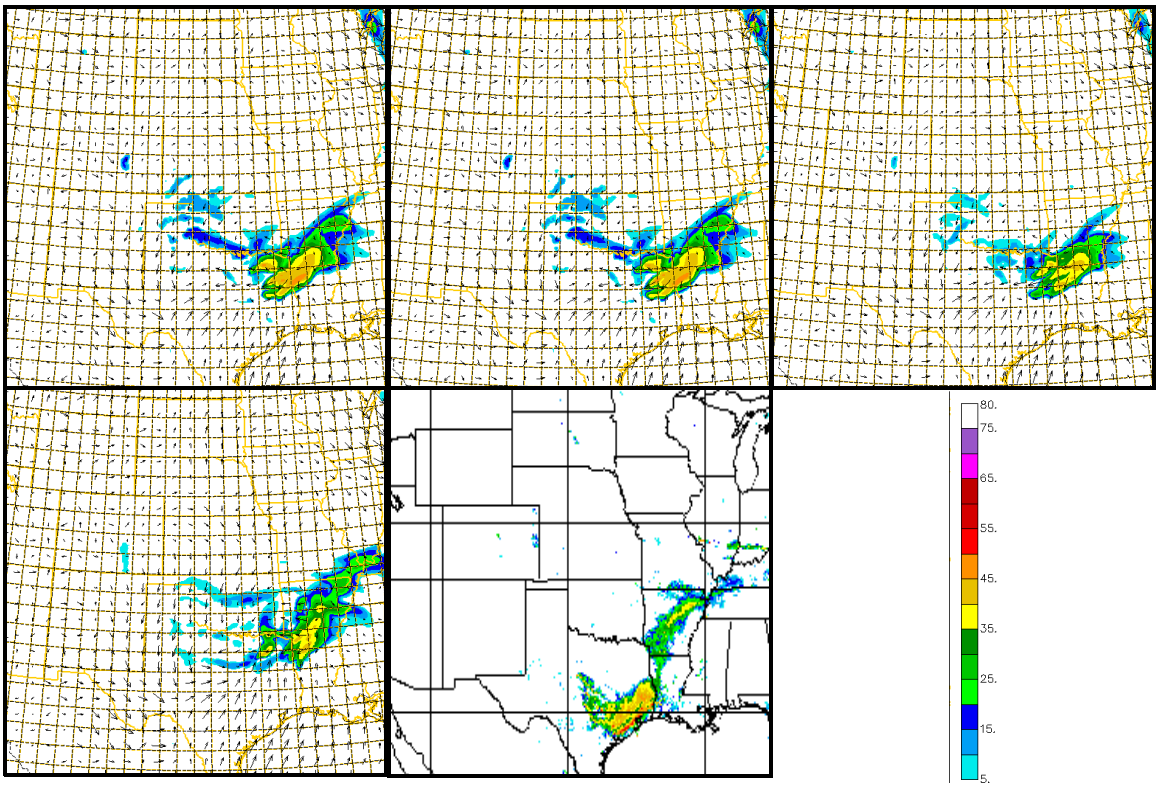

Fig. 5 As in Fig. 3 but for 12Z 16 June 2002 (24 hr forecast)

Figure 6 shows the simulated composite reflectivity for simulation 3km_alldata_c for 3, 12, and 24 hrs into the simulation (top row) along with observed composite reflectivity at the same times (bottom row). It is evident from the figure that this simulation is superior to any of the 9km simulations at capturing both the position (and thus speed) and shape of the MCS. The position errors at 12 and 24 hours are only approximately 50 km and 75 km respectively. Since 3km_alldata used as its initial conditions the interpolated fields from the 9km_alldata simulation, with only an additional cloud analysis performed to take advantage of the higher-resolution radar data (the 9km initial condition already included cloud analysis), the higher resolution and the use of explicit convection in 3km_alldata_c are apparently strong factors in the improved forecast of the MCS over the 9 km resolution simulations. This seems especially true with the ability of this simulation in explicitly resolving the Texas Panhandle convection (visible in the top center panel; compare with the observed convection in the bottom center panel) that is poorly handled by the 9km simulations. Indeed, the overall track of the MCS was improved markedly over the 9km simulations, being overall shifted south and west, closer to the observed track. However, it should be noted that the MCS in this simulation is still slower and is shifted slightly eastward in its track compared to the observations.

3.2 *Precipitation Spectra*

As a further means of analyzing the impact of the mesoscale data and cloud analysis on the prediction of the MCS, power spectra of accumulated precipitation were calculated and compared among the model runs. Future work will include a comparison with observed accumulated precipitation spectra and calculation of power spectra for other quantities. The spectra were calculated by first taking a 2D Fourier transform of the gridded precipitation fields, and then converting the 2D Fourier transformed data into 1D spectra. The spectra for the 9 km domains were calculated only for the area covered by the 3 km domain.

Figure 7 shows 3 hour accumulated precipitation spectra for each of the simulations discussed in this study for the first 3 hours of the simulation. It is within the first few hours that the impact of the cloud analysis might be most clearly seen, and indeed, the simulations that included a cloud analysis, i.e., 9km_alldata_c, and 3km_alldata_c, contain significantly more energy across all wavelengths than the other simulations, indicating increased precipitation at all and more so at smaller scales. Simulation 3km_alldata_c contains significantly more energy in the higher wavenumbers than any of the 9 km simulations, as expected from the higher resolution.

Figure 8 is as Fig. 7 except for the 3 hour accumulated precipitation from 12 to 15 hours into the simulation. By this time, the impact of the cloud analysis has become negligible, with the spectra for 9km_alldata_c virtually identical to that of 9km_alldata. Both of these simulations have slightly more energy in the higher wavenumbers than the other two 9 km simulations, indicating a positive impact of the additional data in the initial conditions. Again, 3km_alldata_c contains significantly more energy in the higher wavenumbers than any of the 9 km simulations at this time as well.

4. SUMMARY AND FUTURE PLAN

The preliminary results discussed herein imply that the use of mesoscale data in addition to the standard NWS data network in the initial conditions may indeed improve forecasts of the MCS. It is also found both by direct examination of the model output fields (such as simulated composite reflectivity) and from accumulated precipitation spectra that for this particular case the use of a complex cloud analysis in the initial conditions has a positive effect on the forecast only for the first few hours of the forecast, after which the effect becomes negligible. Also noted is the overall superiority of the 3 km simulation in the forecast of both the position and shape of the MCS over any of the 9 km simulations. This is most likely due to both the use of explicit convection in this simulation (the 9 km simulations used WRF Kain-Fritsch convective parameterization), as well as the higher horizontal resolution.

Future work will focus 1) on identifying impacts of additional specific high resolution mesoscale data networks on the forecast of the MCS, including those closer to the initiation area of the MCS, 2) the use of different data assimilation strategies, including intermittent assimilation of radar and surface data at small time intervals, and 3) the impact of changes in model computational and physical physical parameters. The model MCS will also be compared more closely with observations, for example by examining the surface wind speeds in the model and comparing to those actually observed with the passage of the MCS, and by determining the pressure difference across the surface cold pool in both the model and observations. The precipitation spectra discussed herein will also be compared with observed precipitation spectra.

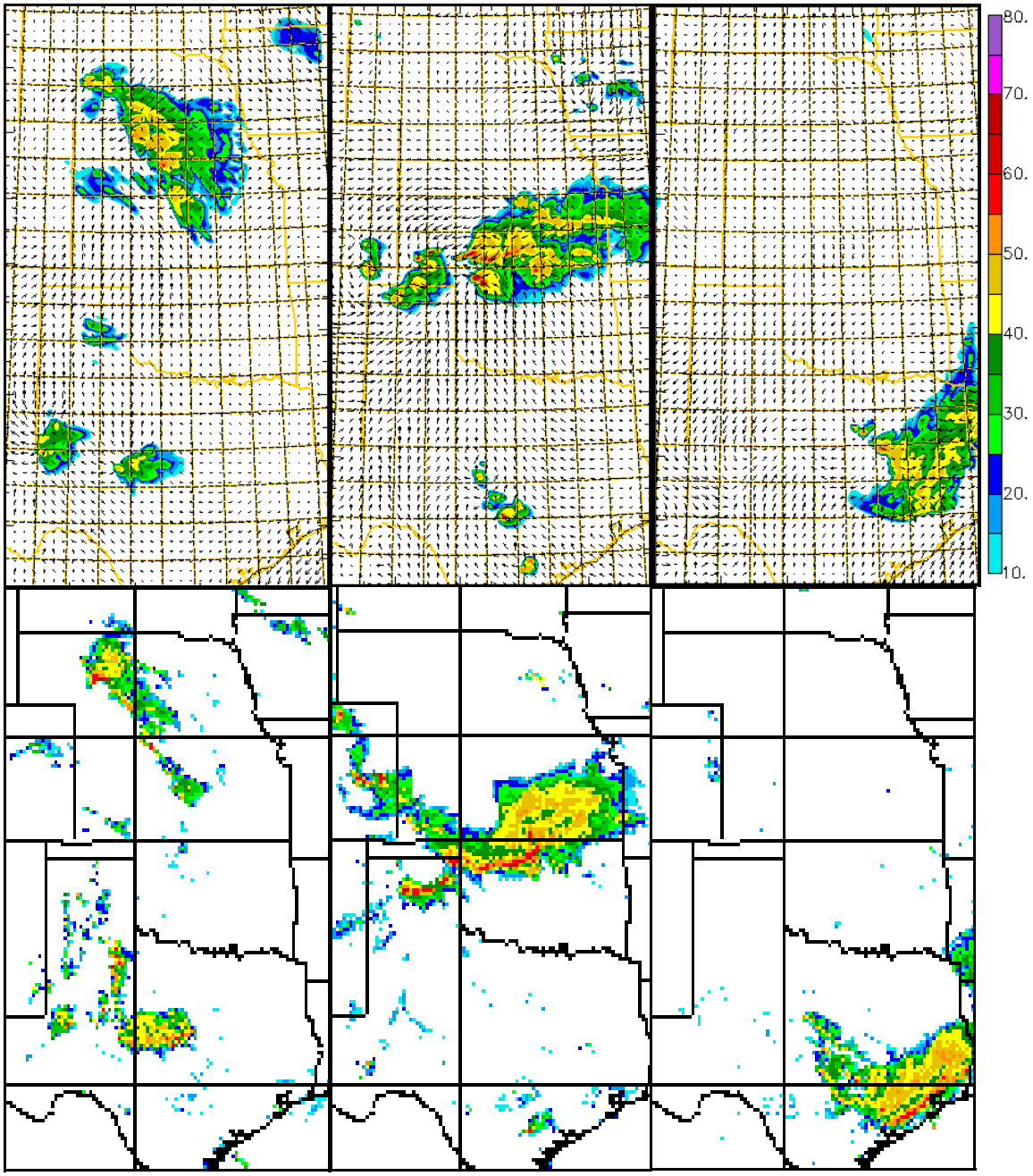

Fig. 6. Simulated composite reflectivity for simulation 3km_alldata_c at 15 Z 15 June 2002 (3 hr forecast, top left), 0Z 16 June 2002 (12 hr forecast, top center), and 12Z 16 June 2002 (24 hr forecast, top right). Observed NEXRAD composite reflectivity at the corresponding times is shown in the bottom row.

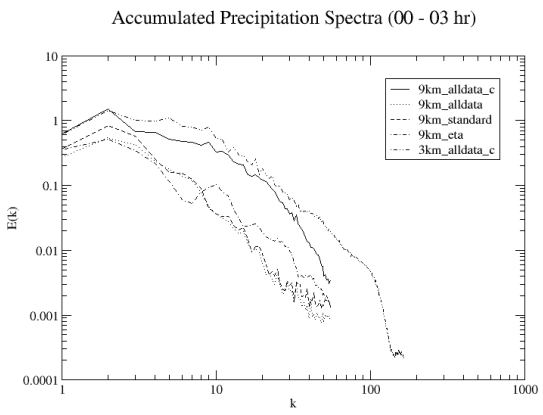

Fig. 7 Accumulated precipitation spectra for forecast hours 00 – 03.

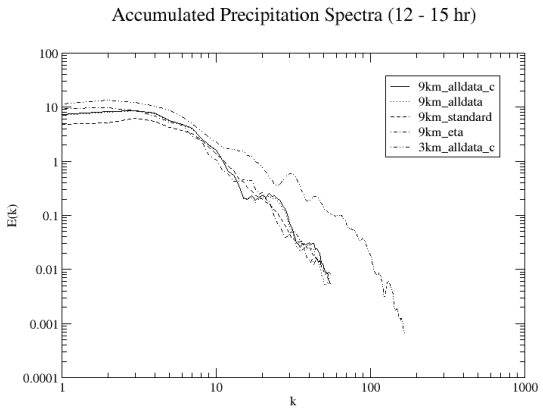

Fig. 8. As in Fig. 7 except for forecast hours 12 – 15.

5. ACKNOWLEDGEMENTS

This work was supported by NSF Grant ATM-0129892 and by the National Defense Science and Engineering Graduate Fellowship awarded to the first author. The authors would like to thank OSCER for the use of its supercomputing facilities during the course of this study.

6. REFERENCES

Brewster, K., 1996: Application of a Bratseth analysis scheme including Doppler radar data. *Preprints, 15th Conf. Wea. Anal. Forecasting*, Norfolk, VA, Amer. Meteor. Soc., 92-95.

Brewster, K. A., 2001a: Phase-correcting data assimilation and application to storm-scale numerical weather prediction. Part I: Method description and simulation testing. *Mon. Wea. Rev.*, **131,** 480-492.

——, 2001b: Phase-correcting data assimilation and application to storm scale numerical weather prediction. Part II: Application to a Severe Storm Outreak. *Mon. Wea. Rev.*, **131,** 493-507.

Case, J. L., J. Manobianco, T. D. Oram, T. Garner, P. F. Blottman, and S. M. Spratt, 2002: Local Data Integration over East-Central Florida Using the ARPS Data Analysis System. *Wea. Forecasting*, **17,** 3-26.

Lazarus, Steven M., Ciliberti, Carol M., Horel, John D., Brewster, Keith A. 2002: Near-Real-Time Applications of a Mesoscale Analysis System to Complex Terrain. *Weather and Forecasting*: Vol. 17, No. 5, pp. 971–1000.

Souto, M. J., C. F. Balseiro, V. Pérez-Muñuzuri, M. Xue, and K. Brewster, 2003: Importance of cloud analysis and impact for daily forecast in terms of climatology of Galician region, Spain. *J. App. Meteor.*, **42,** 129-140.

Xue, M., K. K. Droegemeier, and V. Wong, 2000: The Advanced Regional Prediction System (ARPS) - A multiscale nonhydrostatic atmospheric simulation and prediction tool. Part I: Model dynamics and verification. *Meteor. Atmos. Physics*, **75,** 161-193.

Xue, M., D.-H. Wang, J.-D. Gao, K. Brewster, and K. K. Droegemeier, 2003: The Advanced Regional Prediction System (ARPS), storm-scale numerical weather prediction and data assimilation. *Meteor. Atmos. Physics*, **82,** 139-170.

Xue, M., K. Brewster, D. Weber, K. W. Thomas, F. Kong, and E. Kemp, 2002: Realtime storm-scale forecast support for IHOP 2002 at CAPS. *Preprint, 15th Conf. Num. Wea. Pred. and 19th Conf. Wea. Aanl. Forecasting*, San Antonio, TX, Amer. Meteor. Soc., 124-126.

Zhang, J., F. Carr, and K. Brewster, 1998: ADAS cloud analysis. *Preprints, 12th Conf. on Num. Wea. Pred.*, Phoenix, AZ., Amer. Met. Soc., 185-188.

Zhang, J., 1999: Moisture and Diabatic Initialization Based on Radar and Satellite Observation, School of Meteorology, University of Oklahoma, 194 pp, [Available from School of Meteorology, University of Oklahoma, Norman OK 73019].